Predicting vulnerable sites and causative factors of bank erosion in river Ganga (Malda, India) using remote sensing and statistical modeling approach

DEBARSHI GHOSH (wetlanddeb@gmail.com)
DHUPGURI GIRLS' COLLEGE https://orcid.org/0000-0001-9673-5762
Snehasish Saha
University of North Bengal

Research Article

Keywords: Odds ratio, Log-likelihood statistics, Bank erosion probability, Influential statistics

Posted Date: June 8th, 2022

DOI: https://doi.org/10.21203/rs.3.rs-1636807/v1

Abstract

This study aims to evaluate the causative factors for high bank erosion probability along the left bank of Ganga river in Malda district using binary logistic regression model. The bank erosion at the outer bend of Ganga in Manikchak and Kaliachak-II blocks during the recession of flood water in Ganga poses serious threats to the inhabitants of Diara since the construction of the Farakka barrage. The constriction slowly started a problem of water pilling at the up-stream of the barrage and extended up to the Bhutni Island (40 km up stream). The seepage mechanism allows the entry of rising flood water to the banks and again released when water level recedes gradually and causes bank slumping. In last monsoon (2020), Gopalpur, Jotbhabani Dharampur gram panchayets of Manikchak block are heavily affected by bank erosion. Total nine causative factors are selected as predictor variables in binary logistic regression model categorized broadly as vegetation, water and moisture indices, proximity based on river channel and settlement, soil characteristics and landuse-cover classes. The omnibus test of model coefficient gives the likelihood ratio (224.433) for the overall model fitting (p value 0.0). The model predicts correctly 254 sites as low bank erosion (LBE) and 111 sites as High bank erosion (HBE) category with 84.4% and 67.3% accuracy. The soil bearing capacity significantly expresses highest odds (87.6%) of telling the high probability of bank erosion. The model produces accuracy up to 87.4%.

1. Introduction

The rivers are the lifeline for the survival of mankind on earth. The river operates its normal function of erosion, transportation and deposition in a basin with respect to a base level. Rivers carry out their lives eroding valleys, transporting sediments and forming fluvial sculptures (Ashmore, 2015; M. Singh et al., 2020). The hydro-geomorphic functioning of a river has a potent capability of bringing changes in flow character, erosional-depositional architectures, sediment and ecological regimes (Das, 2019; Hupp et al., 2009; Sinha & Ghosh, 2012). Floodplains and alluvial rivers have been historically and still are one of the most attractive places on Earth for human life and agriculture activities (Allan, 2004; Boix-Fayos et al., 2007; Gordon & Meentemeyer, 2006). The constructions across the rivers bring potential threats to the overall river behavior (M. Biswas & Banerjee, 2018; Tarolli & Sofia, 2016). It increases the chance of sudden changes in the hydraulic geometry of cross sections, depositional character and most importantly the nature of human dependency on rivers (Ortega et al., 2014; Rudorff et al., 2014; Tipa, 2009). In anthropocene era, the man-made changes are inviting large scale devastations within the fluvial systems (Downs & Piégay, 2019; Wohl, 2020). River channel changes, such as bank erosion, down cutting and bank accretion, are natural processes for an alluvial river (Kummu et al., 2008).Bank erosion and channel migration can occur on different timescales (Ahmed & Fawzi, 2011; Bhattacharya et al., 2019; Dotterweich, 2013; Hooke, 2007; Simon & Collison, 2002). Riverbank erosion is not only influenced by climate change, amount of water discharge, type of soil, hydrological and physiological variation, but also anthropological activities, such as different construction along river, dam construction on river, land-use change, etc. (Golfieri et al., 2018; L. Li et al., 2007; S. Roy & Sahu, 2016). River bank erosion is a form of lateral channel expansion as a response to variations in fluid flow and sediment discharges. Lateral migration is therefore a process that can cause catastrophic local or regional changes (J. D. Das et al., 2007; J. D. Das & Saraf, 2007; Pati et al., 2008; Philip et al., 1989; Sinha et al., 2005; Thakur et al., 2012). River Bank shifting is often related to the event where one bank is forming and the opposite bank is eroding (Gazi et al., 2020). Observing the spatiotemporal morpho-dynamics of a river is very crucial to comprehend the river behavior (Leh et al., 2013).The river Ganga forms a marshy flood plain along its course after entering Malda district. As the river passes through different geomorphic characters in the deltaic region, the river repeatedly adjusts itself which leads to erosion and deposition (Nabi et al., 2016). This region is the main playfield of the river and evolved by the successive sedimentation over years and known as Diara. The region covers 1,99,493 hectares and is the result of river laden siltation in the moribund beds of the older Ganga or Mar Ganga (Debanshi & Mandal, 2014). The prolonged sedimentation and consolidation process results in to the formation of Bhutni Island in north-western part of Malda. The tract is supposed to turn into waterlogged flat marshy land considering the old Ganga-Kalindri piracy and mega flood events (Ghosh & Kar, 2018; Mehebub et al., 2015; Sinha & Sarkar, 2009). Severe flood flows of the river water grind down the bank during the monsoon period whereas in the winter, sandbanks become deposited on the both banks of the river.

The Farakka barrage construction commenced in late 1960s and was commissioned in 1975. Since 1975, the upstream river channel has bifurcated into four channels which rejoin together before reaching the barrage and has started meandering in the eastern part (Majumdar & Mandal, 2020a; Mazumder, 2004). In the post barrage period, a deltaic environment suddenly appeared in the upstream part with new adjustment to the artificial base level at Farakka (Islam & Guchhait, 2017; Khatun et al., 2018). It causes the water stagnancy and resultant hydraulic pressure against the river bank along the entire reach which causes repeated river bank failure through subsidence, slumping, toe erosion etc (Rudra, 2020; Thakur et al., 2012). The seepage mechanism allows the entry of rising flood water to the banks and later is released when water level recedes gradually. This process creates many voids in the bank walls and finally causes bank slumping. The erodible sandy composition of the left bank increases risk of bank failure. Thus, the river forms large meander bend at the south of Manikchak block in Malda district. It is a gradual process of the river channel to keep pace with the excess volume of water. The river exhibits a tendency to migrate to east. As a result, many ‘Charlands’ are emerged along the right bank of it (Chakraborty & Pal, 2020; Ullah et al., 2016). Geomorphologically, four channels have developed from west to east. After the construction of the barrage, sequential formation of three channels has been observed. Presently the middle channel is carrying the major flow but before 2006 the eastern most channels used to carry lion share of total river flow. The severity of bank erosion also changes with time here. After 2006, the eastern flow lost its previous flow energy and the main flow started through the central channel (Pal & Pani, 2019; Raj & Singh, 2020). It certainly reduces the high bank erosion at the entire Kaliachak-II and III Blocks (B. Das, 2011). So at present erosion is occurring in that part of left bank of Ganga where main flow through middle channel strikes the concave channel wall. The increased potential energy of the river due to rising water level to the upstream of Farakka barrage is the main cause of accelerated flood and subsequent river bank erosion through meander migration and stream avulsion as the flow has been partially obstructed by the barrage (Mandal, 2017; Thakur et al., 2012). So, bank erosion due to east ward expansion of the channel within the meander belt remains a problem for the inhabitants reside along the left bank. Many scholars from the field of geomorphology have already drawn the attention of international readers considering this prolonged history of river bank erosion in Malda from various angles viz. (i) using Bank Erosion Hazard Index (BEHI) & BANCS model (Majumdar & Mandal, 2020a; Ullah et al., 2016), (ii) using PAR model (R. Biswas & Anwaruzzaman, 2019), (iii) using planform and stream power indices (Majumdar & Mandal, 2020b) and (iv) erosion and LULC dynamicity models (Mandal, 2017; Mondal et al., 2016). In this paper, the authors tried to tie up all the existing research gaps especially the construction of a lucid and holistic model on identification of bank erosion potentials sites after 2020 considering– (i) field visits (ii) remote sensing data (iii) Geographical Information System (GIS) and (iv)regression model.

Remote sensing and GIS in combination can be used to capture empirical responses from historical and current morphological shifts in river channel problems, which would otherwise be challenging to achieve for time and land coverage purposes (Momin et al., 2020). Open-source remote sensing data that allows the rapid identification of morphological changes and how these affect river channels (Langat et al., 2019). Remote sensing and GIS techniques are widely used for the quantification of river bank erosion and change detection of riverbanks worldwide. Several studies have assessed channel change by means of geospatial techniques like time series analysis of different satellite images (Bhuiyan et al., 2017; Dabojani et al., 2014; Downward et al., 1994; Gurnell, 1997; Magliulo et al., 2016; Marston et al., 1995) in diverse categories of river systems. Remote sensing provides a wide scope of spatial modeling, simulation and forecasting of these complex dynamic phenomena with greater accuracy and accountability (Nong & Du, 2011). The spatial model assists the researchers and planners to assess the contemporary issue in hydrological, eco-hydrological modeling and urban planning enables them to predict the probable consequences of spatiotemporal changes of flood discharge, landuse-cover with response to runoff, gulley erosion etc (Arabameri et al., 2018; Mondal & Mandal, 2018) and urban growth (Hamdy et al., 2016; Hou et al., 2019; Mahmoud & Divigalpitiya, 2019; Maithani, 2010; Salem et al., 2019; Sarkar & Chouhan, 2020). Some popular works on soil erosion risk assessment has been done using empirical models like Universal Soil Loss Equation (Roger et al., 2020), the Unit Stream Power Based Erosion/Deposition model (USPED) (Mitas & Mitasova, 1998) and physically based models such as the Water Erosion Prediction Project (Flanagan and Nearing, 1995) (Rawls & Foster, 1987)and the European Soil Erosion Model (Marston et al., 1995; Merritt et al., 2003). While studying bank erosion in Indian and Bangladesh context, most of the research works gave more emphasize on-channel oscillation (Bag et al., 2019; Rudra, 2014; Sarif et al., 2021), bank line shifting (Aher et al., 2012; Gogoi & Goswami, 2014; Mallick & Mallick, 2016) and morpho-dynamics of rivers within the flood plain (Gazi et al., 2020; Nones, 2021; Process et al., 2020). This paper introduces a new angle of identifying potential sites of erosion along a river using combined application of RS and GIS technology.

In this study, the authors have adopted a new technique of bank erosion potential sites identification combining remote sensing and statistical approach. The main objective of this paper is to propose a new remote sensing indices and logistic regression based method for identifying potential sites of bank erosion along the left bank. This modeling has been done by considering nine parameters: i.e., NDVI, Modified NDWI, modified SAVI, modified NDMI, distance to river, distance to settlements, population density, soil dry density, soil bearing capacity and landuse-cover (LULC) categories. The present study also has the objectives of finding the most important causative or driving variable in causing high bank erosion in recent time (2020) using BLR model based on remote sensing data. The use of remotely sensed data in the modeling approach found to be very useful because- (i) the complex role of riparian vegetation adjustment with the soil, (ii) flood inundation (iii) LULC dynamics and (iv) soil characteristics in relation to the bank erosion can easily be included while framing the model. Most importantly, the combination of remote sensing and GIS approach in the first part of the modeling has made the spatial data extraction process much easier for the analyst.

2. Materials And Method

2.1. The study area

The entire region in Malda district of West Bengal is dominantly low-lying and inundation prone in rainy season every year and receives newer alluvium technically called as replenishment. So far as relief is concerned the district is divided into three physical units namely Tal, Diara and Barind (Mistri & Sengupta, 2020). The present study area is highly prone to diluviation and alluviation endeavored by inundations falling within the Diara. Tendering alluviums are dominantly the product of recent Holocene deposits and loosely stratified layers of sands showing interrupted auto-compaction and variegated imprints of cut and fills. The study area comprises of five community development blocks viz. Manikchak, Kaliachak I, Kaliachak II, Kaliachak III and English Bazar (Fig. 1). Among them Manikchak, Kaliachak I, II and III are most affected by outstanding impacts of erosion and instability of the river bank. The western boundary of the district is mostly volatile in view of boundary conditions. The sample sites start from Suksena mouza (mouza; smallest administrative block in India) (Manikchak block) in the upstream and end at Jitmanpur mouza (in Kaliachak-III block) (Figs. 3 & 4). Total 22 mouzas along the left bank of Ganga within a stretch of 55 km are considered in the study to check high bank erosion probability.

2.2. Determination of model parameters and rationale

The prediction of high bank erosion sites along the main channel of Ganga in 2020 is framed on the basis of some raster interpolated indices on pre-defined equations and field-based random sample collection technique (Fig. 2). The selection of driver variables has been fixed on the basis of pilot survey along the left bank of the main channel from 2019 to 2020 in pre and post monsoon times. The spatial variation of the variables is shown within a linear buffer select 6 kms on both sides of the banks. The selected buffer has been clipped with the adjacent mouzas as area feature. The spatial variation has been shown within the limit of the buffer superimposing the clipped mouza boundary layer (Fig. 3). It has kept getting idea on the vulnerable mouzas of high bank erosion (Fig. 4). The pixel radiance values are converted to the Top of Atmospheric reflectance (TOA) corrected bands for Landsat 8 OLI-TIRS sensor data for getting accurate results of various vegetation and water based indices (Novelli & Tarantino, 2015; D. P. Roy et al., 2016; Vanhellemont, 2020). The selected variables have been extracted from the interpolated rasters can be classified into three categories viz. vegetation (Bhandari et al., 2012; Gascon et al., 2016), water and moisture indices rasters (Amani et al., 2016; Bao et al., 2018; Mobasheri & Amani, 2016), proximity rasters (Brennan & Martin, 2012; Demesouka et al., 2013; Zhang et al., 2015) and field collected data based rasters (Table 1). The categorical predictor in the model has been derived from the supervised image classification (8 LULC classes) based on Landsat 8 OLI-TIRS data (2020) using maximum likelihood algorithm in Arc-GIS 10.2.2 platform. The NDVI and MSAVI indices (Mukanov et al., 2019) are considered to check the bank erosion vulnerability at barren and vegetated places (Fig. 6a & b). The MNDWI and NDMI (Fig. 6c & d) are incorporated to know the role of water saturation of bank soil and adjacent floodplain soil either while causing bank erosion (Othman et al., 2014; K. V. Singh et al., 2015). The bank erosion along the abandoned channels, cut-off channel, at the margin of wetlands and swamp tracts can be detected by using MNDWI index. The proximity analysis (Fig. 7a &b) is considered to identify the nearness of main river channel and settlement patches in causing bank erosion. The population density (Fig. 7c) is considered to check the anthropogenic pressure on the river bank (Misra, 2011; Rahman, 2013; Verburg et al., 1999). The field based operation in measuring Soil dry density and bearing capacity both are testified to have what strength as predictor in

causing bank erosion (Chen, 2018; Fragaszy & Lawton, 1984; Gallage & Uchimura, 2010; Liu et al., 2019; Oh & Vanapalli, 2013) (Fig. 8a & b). Finally, the Landuse-cover classes (Fig. 7d) are incorporated in the model as categorical predictor. It reveals the role of changing LULC in aggravating bank erosion or not.

2.3. Explanation of Binary Logistic Regression (BLR) model

In simple linear regression model, the basic assumption is made that the observed data are linearly associated. The assumption is nullified when the researchers are doing work with categorical data. The logarithmic transformation of the normal data presents a way of expressing a non-linear relationship in a linear way. The binary logistic regression is pivoted on expressing the multiple linear regression equation in logarithmic form (Midi et al., 2010; Ozdemir, 2011; Pourghasemi et al., 2013). In this regression, the probability of Y is derived from given known values of X_1 or multiple Xs. The simplest form of the logistic regression from which the probability of Y is to be derived is given in the Eq. 1:

$$P(Y) = \frac{1}{1 + e - (b0 + b1X1i)}$$

1

Where, *P* is the probability of *Y* occurring, *e* is the base of natural logarithms, and the other coefficients are the part of linear combination used in simple linear regression (b_0 is constant, X1 is a predictor variable, b1 is a coefficient). If one wishes to use several predictor variables, the equation becomes:

$$P = \frac{1}{1 + e^{-(b0 + b1X1i + b2X2i + \cdots + bnXni)}} (2)$$

The values of the equation vary from 0 and 1. The value close to 0 means that Y is very unlikely to have occurred and 1 means that Y is very likely to have occurred. In logistic regression, the coefficient (b) attached to every predictor variable (Table 2) is estimated based on maximum likelihood estimator (Gao & Shen, 2007). It helps to select the coefficients that make the observed values most likely to have occurred.

2.4. The log-likelihood statistics

The binary logistic regression model predicts the probability of occurrence of an event (Bera et al., 2020; Lee, 2005). The model gives results in 0 (the outcome didn't occur) and 1 (the outcome did occur). In this model, the log-likelihood statistics is used to assess the fit of the model on the basis of observed and predicted values. The form has been represented in Eq. 3:

$$\log likelihood = \sum_{i=1}^{N} [Yi \ln(P(Yi)) + (1 - Yi) \ln(1 - P(Yi))] (3)$$

The statistics has the capability to sum up the probabilities associated with the predicted and actual outcomes. The log-likelihood statistics is analogous to the residual sum square (SSE) in multiple regression (Hong et al., 2019; Wear & Bolstad, 1998). It is an indicator that how much unexplained variance is there after the model is fitted. The larger value of this statistics indicates a poorly fitted model. In multiple linear regression, the baseline model gives the prediction when we know nothing other than the values of outcome. In logistic regression, the model will predict the outcomes that occur most often.

2.5. Contribution of predictors in the model

In simple linear regression model, the estimated regression coefficient (b) and standard error are derived to compute t-statistics. The aim is to know the individual contribution of each predictor in the model. In logistic regression model, z-statistics is used which follows a normal distribution. It based on the hypothesis that whether the b coefficient for a predictor is significantly different from zero. If the b value significantly differs from zero then the predictor is making a significant contribution to the prediction of the outcome (Y). The z-statistics is known as the Wald statistics (Menard, 2004; Yilmaz, 2009). It sometimes follows the chi-square distribution and becomes z^2. The inflated standard error with high b coefficient value causes underestimation of the Wald statistics.

2.6. Explanation of the odds ratio (exp B)

The odds of an event occurring are defined as the probability of an event occurring to that of the event not occurring. In logistic regression, the odds ratio is the exponential of B and indicates the change in odds resulting from a unit change in the predictor variable (Austin & Steyerberg, 2012; Nemes et al., 2009). It is similar to the b coefficient in the model. The probability (P) of bank erosion with odds of being high or low is shown in the equation number 4 and 5:

$$P(eventhigh) = \frac{1}{1 + e^{-(b0 + b1X1i + b2X2i + \cdots + bnXni}} (4)$$

$$P(eventlow) = 1 - P(eventhigh)$$

5

In this analysis, the bank erosion is to be predicted with 'event high' and 'event low' responses. The equations would like to know-the probability of occurrence of high or low bank erosion from the predictor variables (NDVI, Modified NDWI, modified SAVI, modified NDMI, distance to river, distance to settlements, population density, Soil dry density and finally Soil bearing capacity). In this case, as the predictor variable is dichotomous, our aim is to calculate the odds of finding the site with high erosion (1). The model estimates the probability of the existence of high bank erosion sites based on their driving factors (X) and quantifies the interaction between the existence of high bank erosion and their drivers which are responsible for their occurrences.

2.7. Model validation

The Receiver Operative Characteristic (ROC) compares predicted results with actual results and plot percentages of true positives against the percentage of false positives at a predefined threshold value (Y. Li et al., 2020; Sarkar & Chouhan, 2020). The ROC calculates the area under the curve (AUC), which threshold value lies in between 0 to 1, where 1 denotes a perfect match and 0 denote complete miss-match. The area under curve (AUC) is particularly important for evaluating accuracy of the model(Hu & Lo, 2007; Phillips et al., 2006; Vakhshoori & Zare, 2018). In this study, the probability map of logistic regression is compared to the actual sites of high bank erosion in 2020 to measure the predictability of the model with a threshold value of 0.4. In the BLR model, the smallest cut-off value is the minimum observed test value minus 1 and the largest cutoff value are the maximum observed test value plus 1. Here, we plotted the probability of true positive identified as high bank erosion cells against the probability of the false positive identified as low bank erosion cells for a range of thresholds 0.5–1.The binary classifier has been set to validate two responses like- sites with high bank erosion (1) and low bank erosion (0). The sensitivity (correctly identified sites) of the test can be understood from the Area Under Curve (AUC). AUC is the probability that the model ranks a random positive example more highly than a random negative example. The probability of the classifier to rank the randomly chosen positive values higher than the randomly chosen negative is equal to the probability of AUC. As the AUC goes on increasing above the line of no-discrimination, the probability of correctly defined high bank erosion sites also increases.

3. Results

3.1. The overall model

The comparison of the BLR model has been done with its baseline state when only the constant is included to derive the likelihood ratio which follows the χ^2 distribution. The Cox and Snell R Square 0.382 and Nagelkerke R Square 0.525 indicate suitability of the model (Table 3). The omnibus test of model coefficient gives the likelihood ratio (224.433) for the overall model fitting which is found highly significant (p value 0.000). The overall fitting comes out with the decision that the driver variables are considered to be significant predictors in this model (Table 4). The Hosmer-Lemeshow (HL) test checks weather the observed event rates match with expected event rates or not. The given χ^2 value (4.335) of HL test is found to be significant ($p > 0.005$) (Table 3).The model predicts correctly 254 sites as low bank erosion (LBE) and 111 sites as High bank erosion (HBE) category with 84.4% and 67.3% accuracy. At the same time, the model misclassified 47 sites with HBE and 111 sites with LBE.

3.2. Explaining co linearity diagnostics and residuals

The spatial data modeling with BLR model suffers from a high degree of spatial positive autocorrelation (Sarkar, 2020). The multi-value extraction to point tool in ARC-GIS favours the data extraction process using random point generation. But, random samples are suitable for representing a large number of population data although lacks in eliminating spatial dependency among the random points (Puertas et al. 2014). Both the systematic and random sampling schemes are used to eradicate this problem. The colinearity statistics determined the presence of multi-colinearity among the interpolated raster based indices i.e. NDVI, MNDWI, MSAVI and NDMI with the VIF statistics greater than 10 and tolerance limit less than 0.2. The extracted point data from these raster layers are highly correlated with each other (> 0.8). The trimming of these variables does not make high and influential changes in the odds ratio. So, the acceptability of the overall model has considered here from Hosmer-Lemeshow statistics which confirms the match between the observed and predicted high bank erosion response (1) by the model. The main purpose of examining residuals in any regression model has two objectives: isolating the points for which the model fits poorly and isolating the points that exert an undue influence on the model. The Cook's distance, Leverage statistics and DFBeta values determine the last objective in this model (Fig. 10a, b & c). The standardized residuals of the overall model range between ± 2SD and reveals standard normal distribution of the residuals (Fig. 11a). The shape of the Leverage statistics is observed rightly skewed (3.979) (Fig. 11b). The Cook's distance is calculated less than 1. It indicates that the predictors have influence on the model. The data distribution follows right tailed curve and ranges between 0 to + 0.30 (Fig. 11c). The Expected Leverage Statistics (ELS) is 0.0386 for the overall model. The negative and positive deviations from the expected ELS are 58.58% and 41.42% respectively (Fig. 10d). The DFBeta values for the constant in the model fall below 1.

3.3. Impact of the categorical predictors in the model

In this paper, total 8 landuse-cover categories are used as dummy variables in the BLR model (Fig. 8d). The objective is to find out whether there exists any significant role of any LULC category to predict vulnerable bank erosion sites. Initially, separate BLR model has been run for the LULC classes considering one categorical predictor in the model. The confusion or error matrix is constructed to validate the accuracy of the supervised classification. The Kappa coefficient is 0.765 which agrees 76.5% accuracy of the image classification (Table 5).The overall model indicates the significance of the LULC categorical predictors although with low odd ratio (0.309). The significant z^2statistics (< 0.05) has been calculated for barren lands (Exp(B) 2.272), settlement (Exp(B) 2.897) and swamp tracts (Exp(B) 3.124). The overall accuracy of the BLR model in this case is 64.6%. In both the overall model (16 predictors) and LULC class based model (8 predictors), the barren land category is observed as significant predictor of HBE.

3.4. Validation of the model

Receiver operating characteristic (ROC) curve and Kappa coefficient (Table 5) are used for validation of the BLR model. The kappa coefficient separately approves the accuracy of the image classification. The ROC curve shows the plot of the true positive rate and false positive rate of different likely cut points of a diagnostic test. The Area Under Curve (AUC) determines the goodness of fit of the model. In this study, the probability mapping of vulnerable sites of high bank erosion is compared to the actual training random sample sets fixed both by GPS ground truthing (40%) in 2019 monsoon and random point generator in Arc-GIS platform (60%). The predictability of the model has been tested at 0.4 cutoff point where the model correctly classified 79.4% sites vulnerable to HBE and 21.3% chance of incorrect classification of LBE sites as HBE. The model has the AUC of 0.874 with standard error 0.016 which specifies the selection of vulnerable sites of HBE is valid (Fig. 11e).

4. Discussion

The entire bank line from Manikchak to Farakka is affected by heavy erosion due to unconsolidated and loose constituent bank materials. The entire reach is gradually changing with sand-silt soil resulting into decreasing strength to resist erosion. The left bank erosion of river Ganga has become one of the most severe Geo-hazard in West Bengal. The discussion is framed in such a way so that one can understand about the overall structure of the model at the regional scale. In this paper, the potential sites of bank erosion have been assessed based on the prolonged history of bank erosion in Diara region. It is very essential to present the discussion at reach scale of the river to cross-examine the match of the reality with the model. Previously, Panchanandapur faced the severity of bank erosion (Fig. 5). The pressure of water head in comparison to average cross section area is really an overburden especially at Panchanandapur. The one square meter area receives water head pressure of 2.29 m which is itself a power equals to thousands of hammering against the loose sand-silt composition of the bank soil(Rudra, 2014). Now a days, the severity of bank erosion has been shifted along the outer bank of the meander bend near Gopalpur (Fig. 5). The exertion of water head pressure along the banks can easily exhaust the water saturated loose constituent materials consequent upon steady gravity fall and avalanching of serial blocks of bank soil associated with fissures and gullies. A tremendous head water pressure is predominating at and adjacent to Panchanandapur area up to Farakka. The oversaturated bank soil at the top associated with deep rill and gully formations in monsoon results into steady mud flowage culminating into block failure for the vertical and horizontal fractures (Fig. 6c,e,f). From Manikchak to Panchanandapur, at the outer bend of the curvature of the main central channel is affected by the steady shear stress of impinging water and circulation of revolving or whirling water causes secondary currents (Fig. 6 1e). The thalweg is near to the outer bank (left bank) and very distant from the inner bank. Any bank cannot be protected with embankment pitching and spurs when there is a deep scour depth near the bank (Fig. 6 1c). The loose sand-silt composition attacked by diverted and whirling strikes of impinging ebbs make scars creating crescent cavities of 10–15 m in length observed during the field study in 2019 monsoon.

About 15–20% of population in Manikchak block and about 8678.99 ha have been found under severe threats of erosion. In Kaliachak II about 25–35% of population is under the effect of slumping and disruption of settlements. In English Bazar, about 3–5% population and 483.58 hectare areal coverage have been found under erosional effects. Total 19 mouzas in Manikchak block, 29 mouzas in Kaliachak-II, 4 mouzas of Kaliachak-III and 2 mouzas of English Bazar fall within the selected 6 km buffer along the left bank of Ganga (Fig. 4). Keeping in view the socio-economic strata of the erosion affected areas; increasing population pressure at Bhutni-Diara is another important reason of bank erosion. The island has 3 mouzas and falls in Manikchak block. Bhutni Island had a total population of 89021 according to 2011 census. Previously, it was only 47,173 in 2001. Due to the formation of the circular embankment, the eastern side bank of the river resulting into heavy seasonal slumping alongside for about 15 km starting from Manikchak to Domhat. The increasing population pressure (Table 6) in the adjacent gram panchayet of Manikchak, Englishbazar and Kaliachak-II blocks has direct impact on bank erosion (Fig. 8c). In the categorical predictor model, the settlement LULC class is observed as statistically significant predictor (z^2 statistics less than 0.05) of high bank erosion having an odd ratio of 2.897. It means the 1 square unit increase in settlement patches within the buffer, the log odds of HBE increases by 2.897 times. In the overall model, the euclidean distance from settlement again produces the significant value of z^2 statistics (Table 4). But here the log odds of HBE category decreases by 0.324 with 1 unit increase in distance from settlement. So, the proximity of settlement patches alongside the left bank in Manikchak, Englishbazar and Kaliachak-II are directly and significantly increases the probability of high bank erosion. The river channel category has the highest odd ratio (5.92) among the other categories in LULC classes (Fig. 8d). At 95% confidence level, another LULC class i.e. barren land is considered statistically significant predictor. It indicates the bare land surface in Diara region can easily be engulfed by the lateral erosion of the river Ganga. The NDVI odds 0.203 indicates that 1 unit increase in NDVI value, the odds of HBE decreases by 79.7% (1-0.203). But, the probability is not statistically significant at 95% confidence interval. The increasing distance from main river channel causes the decreasing odds of HBE which is very common. But, another important result comes out from population density variable. It shows that HBE sites (affected mouzas) are 0.677 times less dense than LBE areas.
The measurement of soil bearing capacity is one of the most influencing variables in this model which has direct relationship with the probability of HBE. This measurement is associated with the shear strength of the soil in per square unit area. The shear strength combines frictional resistance and cohesional resistance. Total 50 samples are collected from 25 mouzas covering Manikchak, Kaliachak-II and III blocks (Fig. 1). The mouzas at outer bend of the main channel are having very low soil bearing capacity as the whole water stress falls on the left bank (Fig. 9b). The model tells us that HBE sites are having 0.124 times less soil bearing capacity than the LBE sites and the BLR constant is statistically significant (Table 4). Here, both limits of the confidence interval of the predictor are above 1 gives the inference that the direction of the relationship is true in the population. The bulk density of soil depends greatly on the mineral make up of soil and the degree of compaction. The calculated soil dry density (Fig. 9a) of the bank soil at the study reaches is observed maximum 1.24 g cm^{-3}. The bulk dry density of bank soil is not a significant predictor in the overall model. But if one uses this as single predictor in BLR model, the b-constant becomes-0.844 with an odd ratio of 0.430 and it becomes statistically significant. The model has been constructed to snap the role of- complex interaction of the selected parameters in the model and find out the most crucial parameter which has relatively high probability of predicting bank erosion. The remote sensing tool helped to understand the complex interaction of LULC and riparian soil-vegetation assemblage in the model with the odds explained in Table 4. Interestingly, the log odd of HBE probability is comparatively higher for the 1 unit change in agricultural fields in LULC category. The spatial distribution of probability scores (HBE) indicates the good fit of the BLR model along the outer bend of the main channel in Diara (Fig. 12a). The high probability scores concentrated around the large meandering curvature especially at Dharampur (Fig. 12b), Jotbhabani (Fig. 12c), Gopalpur (Fig. 12d), Kamaluddinpur (Fig. 12e), Mahadebpur mouzas (Fig. 12f &G). These sites bear the recent (2020) flood hit and related architectures of bank erosion.

The model predicts the chance of more bank erosion in agricultural field dominated riparian sites. Finally, the model has presented the capability of advanced remote sensing and GIS technology to predict bank erosion considering the complex interaction of the riparian zone.

5. Conclusion

The present study reveals the applicability BRL model in predicting high vulnerable sites for bank erosion. The model uses causative variables that were collected from different spectrum i.e. field based and raster grid bases. The NDVI, MNDWI, MSAVI and NDMI indices are used in this vulnerability prediction modeling approach with their inherent capability of spatial allocation and detecting intensive patches. The model holds the possibility of predicting the role of LULC categories in bank erosion. It inevitably draws the significant dynamic role of spatial pattern and association of LULC categories. The model figures out the role of nearness of the river channel to settlement patches promoting anthropogenic pressure on the already vulnerable sites. It contradictorily reveals the

consensus of people to live away from vulnerable sites especially the urban areas. The intensity of bank erosion is undoubtedly connected with the construction of Farakka barrage and frequent oscillation of the main channel of Ganga. The large bend of the present channel at Manichak and Kaliachak-II block is the morphological adjustment of the channel in post Farakka barrage time. The moist low lands of Diara favours the lateral expansion of the channel to the east. The left bank from Dharampur to Hamidpur is highly affected by irregular water regimes in wet and dry seasons as well water currents during high spates. From Paschim Narayanpur to Gopalpur (Manikchak) the bank soil bearing capacity is observed low. The BLR model also predicts the high probability of bank erosion (> 90%) within Paschim Narayanpur (Manikchak) to Jotananta (Kaliachak-II). Below this the high probability only can be observed as scattered patches within Panchanandapur, Hamidpur and Nayagram (Kaliachak-II). After 2007 the degree of severity of erosion has been found comparatively dormant here. The swamp tracts of Bhuti-Diara Island are highly vulnerable to bank erosion. The agricultural fields in Kaliachak-II and III are being rapidly engulfed by the seasonal flood devastations promoting bank erosion. The present paper does not claim the direct population pressure on the left bank. It perceives the rapid conversion of agricultural fields and mango plantations to settlement patches as a result of LULC dynamics. The soil bearing capacity significantly expresses 87.6% odds of telling high probability of bank erosion which is highest among non-categorical predictors. The increasing proximity of settlement patches increases the probability of HBE which is indirectly related to the bank erosion. The population density variable in BLR model indicates the adaptation of human settlements with bank erosion. The HBE sites lead to drive them away from to find more suitable lands in the interior part of Diara. Finally, the model produces accuracy up to 87.4% to produce overall impact of the driving variables nullifying the problem of spatial autocorrelation.

Declarations

Declaration of the conflict of interest (COI)

The authors by any means intentionally do not attract any common interest towards conflict neither they mutually have any COI nor any community or group of people on their part.

Availability of data and material

Not applicable for this article.

Funding

This article is sponsored by the Dept. of Science & Technology, Govt. of West Bengal as a Major research Project.

Authors' contributions

Debarshi Ghosh (first author): Field data collection, data compilation, writing the methodology, RS-GIS support, writing the draft.

Dr. Snehasish Saha (second author): Finalizing the manuscript, overall supervision.

Acknowledgements

The authors are greatly thankful to Mr. Kunal Chakraborty, Research Scholar, Dept. of Geography, University of North Bengal for his inspiring support in accomplishing the field work. We also wish to admit the technical help received from the senior scientists of DST, Govt. of WB.

References

1. Aher SP, Bairagi SI, Deshmukh PP, Gaikwad RD (2012) ISSN: 2249 – 0868 Foundation of Computer Science FCS. Int J Appl Inform Syst (IJAIS) 2(3):1–7 www.ijais.org
2. Ahmed AA, Fawzi A (2011) Meandering and bank erosion of the River Nile and its environmental impact on the area between Sohag and El-Minia, Egypt. Arab J Geosci 4(1):1–11. https://doi.org/10.1007/s12517-009-0048-y
3. Allan JD (2004) Landscapes and riverscapes: The influence of land use on stream ecosystems. *Annual Review of Ecology, Evolution, and Systematics*, *35*(2002), 257–284. https://doi.org/10.1146/annurev.ecolsys.35.120202.110122
4. Amani M, Parsian S, MirMazloumi SM, Aieneh O (2016) Two new soil moisture indices based on the NIR-red triangle space of Landsat-8 data. Int J Appl Earth Obs Geoinf 50:176–186. https://doi.org/10.1016/j.jag.2016.03.018
5. Arabameri A, Pradhan B, Rezaei K, Yamani M, Pourghasemi HR, Lombardo L (2018) Spatial modelling of gully erosion using evidential belief function, logistic regression, and a new ensemble of evidential belief function–logistic regression algorithm. Land Degrad Dev 29(11):4035–4049. https://doi.org/10.1002/ldr.3151
6. Ashmore P (2015) Towards a sociogeomorphology of rivers. Geomorphology 251:149–156. https://doi.org/10.1016/j.geomorph.2015.02.020
7. Austin PC, Steyerberg EW (2012) Interpreting the concordance statistic of a logistic regression model: Relation to the variance and odds ratio of a continuous explanatory variable. BMC Med Res Methodol 12:1–8. https://doi.org/10.1186/1471-2288-12-82
8. Bag R, Mondal I, Bandyopadhyay J (2019) Assessing the oscillation of channel geometry and meander migration cardinality of Bhagirathi River, West Bengal, India. J Geog Sci 29(4):613–634. https://doi.org/10.1007/s11442-019-1618-z
9. Bao Y, Lin L, Wu S, Kwal Deng KA, Petropoulos GP (2018) Surface soil moisture retrievals over partially vegetated areas from the synergy of Sentinel-1 and Landsat 8 data using a modified water-cloud model. Int J Appl Earth Obs Geoinf 72(May):76–85. https://doi.org/10.1016/j.jag.2018.05.026

10. Bera B, Saha S, Bhattacharjee S (2020) Forest cover dynamics (1998 to 2019) and prediction of deforestation probability using binary logistic regression (BLR) model of Silabati watershed, India. Trees Forests and People 2(September):100034. https://doi.org/10.1016/j.tfp.2020.100034
11. Bhandari AK, Kumar A, Singh GK (2012) Feature Extraction using Normalized Difference Vegetation Index (NDVI): A Case Study of Jabalpur City. Procedia Technol 6:612–621. https://doi.org/10.1016/j.protcy.2012.10.074
12. Bhattacharya RK, Chatterjee D, Das K (2019) Geomorphic response to riverine land cover dynamics in a quarried alluvial river Kangsabati, South Bengal, India. Environ Earth Sci 78(22). https://doi.org/10.1007/s12665-019-8652-y
13. Bhuiyan MAH, Islam SMD-U, Azam G (2017) Exploring impacts and livelihood vulnerability of riverbank erosion hazard among rural household along the river Padma of Bangladesh. Environ Syst Res 6(1). https://doi.org/10.1186/s40068-017-0102-9
14. Biswas M, Banerjee P (2018) Bridge construction and river channel morphology—A comprehensive study of flow behavior and sediment size alteration of the River Chel, India. Arab J Geosci 11(16). https://doi.org/10.1007/s12517-018-3789-7
15. Biswas R, Anwaruzzaman AKM (2019) Measuring Hazard Vulnerability by Bank Erosion of the Ganga River in Malda District Using PAR Model. J Geogr Environ Earth Sci Int 1–15. https://doi.org/10.9734/jgeesi/2019/v22i130136
16. Boix-Fayos C, Barberá GG, López-Bermúdez F, Castillo VM (2007) Effects of check dams, reforestation and land-use changes on river channel morphology: Case study of the Rogativa catchment (Murcia, Spain). Geomorphology 91(1–2):103–123. https://doi.org/10.1016/j.geomorph.2007.02.003
17. Brennan J, Martin E (2012) Spatial proximity is more than just a distance measure. Int J Hum Comput Stud 70(1):88–106. https://doi.org/10.1016/j.ijhcs.2011.08.006
18. Chakraborty R, Pal S (2020) Application of numerical models to simulate the charland area from Rajmahal to Farakka barrage of the Ganga river of eastern India. Spat Inform Res 28(6):683–698. https://doi.org/10.1007/s41324-020-00327-9
19. Chen Y (2018) Soil–Water Retention Curves Derived as a Function of Soil Dry Density. GeoHazards 1(1):3–19. https://doi.org/10.3390/geohazards1010002
20. Dabojani D, Mithun D, Kanti KK (2014) River Change Detection and Bankline Erosion Recognition using Remote Sensing and GIS. *Forum Geografic*, *XIII*(1), 12–17. https://doi.org/10.5775/fg.2067-4635.2014.038.i
21. Das B (2011) Stakeholders' perception in identification of river bank erosion hazard: A case study. Nat Hazards 58(3):905–928. https://doi.org/10.1007/s11069-010-9698-z
22. Das JD, Dutta T, Saraf AK (2007) Remote sensing and GIS application in change detection of the Barak River channel, N.E. India. J Indian Soc Remote Sens 35(4):301–312. https://doi.org/10.1007/BF02990786
23. Das JD, Saraf AK (2007) Remote sensing in the mapping of the Brahmaputra/Jamuna River channel patterns and its relation to various landforms and tectonic environment. Int J Remote Sens 28(16):3619–3631. https://doi.org/10.1080/01431160601009664
24. Das S (2019) Geospatial mapping of flood susceptibility and hydro-geomorphic response to the floods in Ulhas basin, India. *Remote Sensing Applications: Society and Environment*, *14*(September 2018), 60–74. https://doi.org/10.1016/j.rsase.2019.02.006
25. Debanshi J, Mandal S (2014) Dynamicity of the River Ganga and Bank Erosion Induced Land Loss in Manikchak Diara of Malda District of West Bengal, India: A RS and GIS based Geo. Int J Appl Remote Sens GIS 3(1):43–56. https://www.researchgate.net/profile/Sujit_Mandal3/publication/309322157_Dynamicity_of_the_River_Ganga_and_Bank_Erosion_Induced_Land_Loss_in_spatial_approach/links/5809fffa08ae4
26. Demesouka OE, Vavatsikos AP, Anagnostopoulos KP (2013) Suitability analysis for siting MSW landfills and its multicriteria spatial decision support system: Method, implementation and case study. Waste Manag 33(5):1190–1206. https://doi.org/10.1016/j.wasman.2013.01.030
27. Dotterweich M (2013) The history of human-induced soil erosion: Geomorphic legacies, early descriptions and research, and the development of soil conservation-A global synopsis. Geomorphology 201:1–34. https://doi.org/10.1016/j.geomorph.2013.07.021
28. Downs PW, Piégay H (2019) Catchment-scale cumulative impact of human activities on river channels in the late Anthropocene: implications, limitations, prospect. Geomorphology 338:88–104. https://doi.org/10.1016/j.geomorph.2019.03.021
29. Downward SR, Gurnell AM, Brookes A (1994) A methodology for quantifying river channel planform change using GIS. *Variability in Stream Erosion and Sediment Transport. Proc. Symposium, Canberrra, 1994*, *224*, 449–456
30. Fragaszy RJ, Lawton E (1984) Bearing capacity of reinforced sand subgrades. J Geotech Eng 110(10):1500–1507. https://doi.org/10.1061/(ASCE)0733-9410(1984)110:10(1500)
31. Gallage CPK, Uchimura T (2010) Effects of dry density and grain size distribution on soil-water characteristic curves of sandy soils. Soils Found 50(1):161–172. https://doi.org/10.3208/sandf.50.161
32. Gao S, Shen J (2007) Asymptotic properties of a double penalized maximum likelihood estimator in logistic regression. Stat Probab Lett 77(9):925–930. https://doi.org/10.1016/j.spl.2007.01.004
33. Gascon M, Cirach M, Martínez D, Dadvand P, Valentín A, Plasència A, Nieuwenhuijsen MJ (2016) Normalized difference vegetation index (NDVI) as a marker of surrounding greenness in epidemiological studies: The case of Barcelona city. Urban Forestry and Urban Greening 19:88–94. https://doi.org/10.1016/j.ufug.2016.07.001
34. Gazi MY, Hossain F, Sadeak S, Uddin MM (2020) Spatiotemporal variability of channel and bar morphodynamics in the Gorai-Madhumati River, Bangladesh using remote sensing and GIS techniques. Front Earth Sci 14(4):828–841. https://doi.org/10.1007/s11707-020-0827-z
35. Ghosh A, Kar SK (2018) Application of analytical hierarchy process (AHP) for flood risk assessment: a case study in Malda district of West Bengal, India. Nat Hazards 94(1):349–368. https://doi.org/10.1007/s11069-018-3392-y

36. Gogoi C, Goswami DC (2014) A study on channel migration of the subansiri river in assam using remote sensing and gis technology. Curr Sci 106(8):1113–1120. https://doi.org/10.18520/cs/v106/i8/1113-1120
37. Golfieri B, Surian N, Hardersen S (2018) Towards a more comprehensive assessment of river corridor conditions: A comparison between the Morphological Quality Index and three biotic indices. *Ecological Indicators*, *84*(September 2017), 525–534. https://doi.org/10.1016/j.ecolind.2017.09.011
38. Gordon E, Meentemeyer RK (2006) Effects of dam operation and land use on stream channel morphology and riparian vegetation. Geomorphology 82(3–4):412–429. https://doi.org/10.1016/j.geomorph.2006.06.001
39. Hamdy O, Zhao S, Osman T, Salheen MA, Eid YY (2016) Applying a hybrid model of markov chain and logistic regression to identify future urban sprawl in abouelreesh, aswan: A case study. Geosci (Switzerland) 6(4). https://doi.org/10.3390/geosciences6040043
40. Hong H, Jaafari A, Zenner EK (2019) Predicting spatial patterns of wildfire susceptibility in the Huichang County, China: An integrated model to analysis of landscape indicators. Ecol Ind 101(January):878–891. https://doi.org/10.1016/j.ecolind.2019.01.056
41. Hooke JM (2007) Spatial variability, mechanisms and propagation of change in an active meandering river. Geomorphology 84(3–4):277–296. https://doi.org/10.1016/j.geomorph.2006.06.005
42. Hou H, Wang R, Murayama Y (2019) Scenario-based modelling for urban sustainability focusing on changes in cropland under rapid urbanization: A case study of Hangzhou from 1990 to 2035. Sci Total Environ 661:422–431. https://doi.org/10.1016/j.scitotenv.2019.01.208
43. Hu Z, Lo CP (2007) Modeling urban growth in Atlanta using logistic regression. Comput Environ Urban Syst 31(6):667–688. https://doi.org/10.1016/j.compenvurbsys.2006.11.001
44. Hupp CR, Pierce AR, Noe GB (2009) Floodplain geomorphic processes and environmental impacts of human alteration along coastal plain rivers. USA Wetlands 29(2):413–429. https://doi.org/10.1672/08-169.1
45. Islam A, Guchhait SK (2017) Analysing the influence of Farakka Barrage Project on channel dynamics and meander geometry of Bhagirathi river of West Bengal, India. Arab J Geosci 10(11). https://doi.org/10.1007/s12517-017-3004-2
46. Khatun S, Das S, Pal S (2018) Exploring the ambient environment for charland formation in Rajmahal downstream Ganga river of Eastern India in post Farakka barrage Period. Spat Inform Res 26(3):337–346. https://doi.org/10.1007/s41324-018-0179-x
47. Kummu M, Lu XX, Rasphone A, Sarkkula J, Koponen J (2008) Riverbank changes along the Mekong River: Remote sensing detection in the Vientiane-Nong Khai area. Quatern Int 186(1):100–112. https://doi.org/10.1016/j.quaint.2007.10.015
48. Langat PK, Kumar L, Koech R (2019) Monitoring river channel dynamics using remote sensing and GIS techniques. Geomorphology 325:92–102. https://doi.org/10.1016/j.geomorph.2018.10.007
49. Lee S (2005) Application of logistic regression model and its validation for landslide susceptibility mapping using GIS and remote sensing data. Int J Remote Sens 26(7):1477–1491. https://doi.org/10.1080/01431160412331331012
50. Leh M, Bajwa S, Chaubey I (2013) IMPACT of land use change on erosion risk: AN integrated remote sensing, geographic information system and modeling methodology. Land Degrad Dev 24(5):409–421. https://doi.org/10.1002/ldr.1137
51. Li L, Lu XX, Chen Z (2007) River channel change during the last 50 years in the middle Yangtze River, the Jianli reach. Geomorphology 85(3–4):185–196. https://doi.org/10.1016/j.geomorph.2006.03.035
52. Li Y, Liu X, Han Z, Dou J (2020) Spatial proximity-based geographically weighted regression model for landslide susceptibility assessment: A case study of Qingchuan area, China. Appl Sci (Switzerland) 10(3). https://doi.org/10.3390/app10031107
53. Liu H, Wang C, long, Kong G, qiang, Bouazza A (2019) Ultimate bearing capacity of energy piles in dry and saturated sand. Acta Geotech 14(3):869–879. https://doi.org/10.1007/s11440-018-0661-6
54. Magliulo P, Bozzi F, Pignone M (2016) Assessing the planform changes of the Tammaro River (southern Italy) from 1870 to 1955 using a GIS-aided historical map analysis. Environ Earth Sci 75(4):1–19. https://doi.org/10.1007/s12665-016-5266-5
55. Mahmoud H, Divigalpitiya P (2019) Spatiotemporal variation analysis of urban land expansion in the establishment of new communities in Upper Egypt: A case study of New Asyut city. Egypt J Remote Sens Space Sci 22(1):59–66. https://doi.org/10.1016/j.ejrs.2018.03.006
56. Maithani S (2010) Cellular Automata Based Model of Urban Spatial Growth. J Indian Soc Remote Sens 38(4):604–610. https://doi.org/10.1007/s12524-010-0053-3
57. Majumdar S, Mandal S (2020a) Acceptance of BANCS model for predicting stream bank erosion potential and rate in the left bank of Ganga river of Diara region in Malda district, North East India. Spat Inform Res. https://doi.org/10.1007/s41324-020-00334-w
58. Majumdar S, Mandal S (2020b) Assessment of relationship of braiding intensities with stream power and bank erosion rate through Plan Form Index (PFI) method: a study on selected reaches of the upstream of Ganga river near Malda district, West Bengal, India. Sustainable Water Resources Management 6(6). https://doi.org/10.1007/s40899-020-00462-z
59. Mallick S, Mallick S (2016) Identification of Fluvio-Geomorphological Changes and Bank Line Shifting of River Bhagirathi-Hugli Using Remote Sensing Technique in and Around of Mayapur Nabadwip Area, West Bengal. Int J Sci Res (IJSR) 5(3):1130–1134. https://doi.org/10.21275/v5i3.nov162080
60. Mandal S (2017) Assessing the instability and shifting character of the river bank Ganga In Manikchak Diara Of Malda District, West Bengal Using Bank Erosion Hazard Index (BEHI), RS & GIS. Eur J Geogr 8(4):6–25
61. Marston RA, Girel J, Pautou G, Piegay H, Bravard JP, Arneson C (1995) Channel metamorphosis, floodplain disturbance, and vegetation development: Ain River, France. Geomorphology 13(1–4):121–131. https://doi.org/10.1016/0169-555X(95)00066-E
62. Mazumder SK (2004) *Role of Farakka Barrage on the Disastrous 1998 Flood in Malda (West Bengal). Icid*, 39–48. https://doi.org/10.1007/978-1-4020-2792-5_3

63. Mehebub S, Raihan A, Nuhul H, Haroon S (2015) Assessing flood inundation extent and landscape vulnerability to flood using geospatial technology: A study of Malda district of West Bengal, India. Forum Geografic XIV(2):156–163. https://doi.org/10.5775/fg.2067-4635.2015.144.d
64. Menard S (2004) Six approaches to calculating standardized logistic regression coefficients. Am Stat 58(3):218–223. https://doi.org/10.1198/000313004X946
65. Merritt WS, Letcher RA, Jakeman AJ (2003) A review of erosion and sediment transport models. Environ Model Softw 18(8–9):761–799. https://doi.org/10.1016/S1364-8152(03)00078-1
66. Midi H, Sarkar SK, Rana S (2010) Collinearity diagnostics of binary logistic regression model. J Interdisciplinary Math 13(3):253–267. https://doi.org/10.1080/09720502.2010.10700699
67. Misra AK (2011) Impact of Urbanization on the Hydrology of Ganga Basin (India). Water Resour Manage 25(2):705–719. https://doi.org/10.1007/s11269-010-9722-9
68. Mistri P, Sengupta S (2020) Multi-criteria Decision-Making Approaches to Agricultural Land Suitability Classification of Malda District, Eastern India. Nat Resour Res 29(3):2237–2256. https://doi.org/10.1007/s11053-019-09556-8
69. Mitas L, Mitasova H (1998) Distributed erosion modeling for effective erosion prevention. Water Resour Res 34(3):505–516
70. Mobasheri MR, Amani M (2016) Soil moisture content assessment based on Landsat 8 red, near-infrared, and thermal channels. J Appl Remote Sens 10(2):026011. https://doi.org/10.1117/1.jrs.10.026011
71. Momin H, Biswas R, Tamang C (2020) Morphological analysis and channel shifting of the Fulahar river in Malda district, West Bengal, India using remote sensing and GIS techniques. GeoJournal 7 (Chang 2008. https://doi.org/10.1007/s10708-020-10248-7
72. Mondal J, Debanshi S, Mandal S (2016) *Dynamicity of the River Ganga and Bank Erosion Induced Land Loss in Dynamicity of the River Ganga and Bank Erosion Induced Land Loss in Manikchak Diara of Malda District of West Bengal, India : A RS and GIS based Geo-spatial approach*. *June*
73. Mondal J, Mandal S (2018) Monitoring changing course of the river Ganga and land-use dynamicity in Manikchak Diara of Malda district, West Bengal, India, using geospatial tools. Spat Inform Res 26(6):691–704. https://doi.org/10.1007/s41324-018-0210-2
74. Mukanov Y, Chen Y, Baisholanov S, Amanambu AC, Issanova G, Abenova A, Fang G, Abayev N (2019) Estimation of annual average soil loss using the Revised Universal Soil Loss Equation (RUSLE) integrated in a Geographical Information System (GIS) of the Esil River basin (ERB), Kazakhstan. Acta Geophys 67(3):921–938. https://doi.org/10.1007/s11600-019-00288-0
75. Nabi MR, Rashid MS, Hossain MI (2016) Historical Bankline Shifting Since 1760s: A GIS and Remote Sensing Based Case Study of Meghna River Plate of Rennell's Atlas. Int J Sci Res Publications 6(12):473–483 www.ijsrp.org
76. Nemes S, Jonasson JM, Genell A, Steineck G (2009) Bias in odds ratios by logistic regression modelling and sample size. BMC Med Res Methodol 9(1):1–5. https://doi.org/10.1186/1471-2288-9-56
77. Nones M (2021) Remote sensing and GIS techniques to monitor morphological changes along the middle-lower Vistula river, Poland. Int J River Basin Manage 19(3):345–357. https://doi.org/10.1080/15715124.2020.1742137
78. Nong Y, Du Q (2011) Urban growth pattern modeling using logistic regression. Geo-Spatial Inform Sci 14(1):62–67. https://doi.org/10.1007/s11806-011-0427-x
79. Novelli A, Tarantino E (2015) Combining ad hoc spectral indices based on LANDSAT-8 OLI/TIRS sensor data for the detection of plastic cover vineyard. Remote Sens Lett 6(12):933–941. https://doi.org/10.1080/2150704X.2015.1093186
80. Oh WT, Vanapalli SK (2013) Interpretation of the Bearing Capacity of Unsaturated Fine-Grained Soil Using the Modified Effective and the Modified Total Stress Approaches. Int J Geomech 13(6):769–778. https://doi.org/10.1061/(asce)gm.1943-5622.0000263
81. Ortega JA, Razola L, Garzón G (2014) Recent human impacts and change in dynamics and morphology of ephemeral rivers. Nat Hazards Earth Syst Sci 14(3):713–730. https://doi.org/10.5194/nhess-14-713-2014
82. Othman AA, Al-Saady YI, Al-Khafaji AK, Gloaguen R (2014) Environmental change detection in the central part of Iraq using remote sensing data and GIS. Arab J Geosci 7(3):1017–1028. https://doi.org/10.1007/s12517-013-0870-0
83. Ozdemir A (2011) Using a binary logistic regression method and GIS for evaluating and mapping the groundwater spring potential in the Sultan Mountains (Aksehir, Turkey). J Hydrol 405(1–2):123–136. https://doi.org/10.1016/j.jhydrol.2011.05.015
84. Pal R, Pani P (2019) Remote sensing and GIS-based analysis of evolving planform morphology of the middle-lower part of the Ganga River, India. Egypt J Remote Sens Space Sci 22(1):1–10. https://doi.org/10.1016/j.ejrs.2018.01.007
85. Pati JK, Lal J, Prakash K, Bhusan R (2008) Spatio-temporal shift of western bank of the Ganga river, Allahabad city and its implications. J Indian Soc Remote Sens 36(3):289–297. https://doi.org/10.1007/s12524-008-0030-2
86. Philip G, Gupta RP, Bhattacharya A (1989) Channel migration studies in the middle ganga basin, india, using remote sensing data. Int J Remote Sens 10(6):1141–1149. https://doi.org/10.1080/01431168908903953
87. Phillips SB, Aneja VP, Kang D, Arya SP (2006) Modelling and analysis of the atmospheric nitrogen deposition in North Carolina. Int J Global Environ Issues 6(2–3):231–252. https://doi.org/10.1016/j.ecolmodel.2005.03.026
88. Pourghasemi HR, Moradi HR, Fatemi Aghda SM (2013) Landslide susceptibility mapping by binary logistic regression, analytical hierarchy process, and statistical index models and assessment of their performances. Nat Hazards 69(1):749–779. https://doi.org/10.1007/s11069-013-0728-5
89. Process H, Sarkar A, Secondary CA, Author C, Ghosh D, Sarkar A, Ghosh D (2020) *GeoJournal Spatial modeling of avulsion potential zones in lower catchment of Chel River, North Bengal (India) using Fuzzy logic & Multi-Criteria Evaluation technique Spatial modeling of avulsion potential zones in lower catchment of Chel River, North*

90. Rahman M (2013) Impact of Riverbank Erosion Hazard in the Jamuna Floodplain Areas in Bangladesh. J Sci Foundation 8(1–2):55–65. https://doi.org/10.3329/jsf.v8i1-2.14627
91. Raj C, Singh V (2020) Assessment of planform changes of the Ganga River from Bhagalpur to Farakka during 1973–2019 using satellite imagery. ISH J Hydraulic Eng 00(00):1–11. https://doi.org/10.1080/09715010.2020.1812123
92. Rawls WJ, Foster GR (1987) *Usda-Water Erosion Prediction Project (Wepp). July*, 702–707
93. Roger J, Herbert B, Kenneth G (2020) *Application of the USLE to Southwestern Rangelands Download date Link to Item Hydrology and Water Resources in Arizona and the Southwest*
94. Roy DP, Kovalskyy V, Zhang HK, Vermote EF, Yan L, Kumar SS, Egorov A (2016) Characterization of Landsat-7 to Landsat-8 reflective wavelength and normalized difference vegetation index continuity. Remote Sens Environ 185:57–70. https://doi.org/10.1016/j.rse.2015.12.024
95. Roy S, Sahu AS (2016) Effect of land cover on channel form adjustment of headwater streams in a lateritic belt of West Bengal (India). Int Soil Water Conserv Res 4(4):267–277. https://doi.org/10.1016/j.iswcr.2016.09.002
96. Rudorff CM, Melack JM, Bates PD (2014) Flooding dynamics on the lower Amazon floodplain: 2. Seasonal and interannual hydrological variability. Water Resour Res 50(1):635–649. https://doi.org/10.1002/2013WR014714
97. Rudra K (2010) Dynamics of the Ganga in West Bengal, India (1764–2007): Implications for science-policy interaction. Quatern Int 227(2):161–169. https://doi.org/10.1016/j.quaint.2009.10.043
98. Rudra K (2014) Changing river courses in the western part of the Ganga-Brahmaputra delta. Geomorphology 227:87–100. https://doi.org/10.1016/j.geomorph.2014.05.013
99. Rudra K (2020) Disaster Studies. In *Disaster Studies*. Springer Singap. https://doi.org/10.1007/978-981-32-9339-7
100. Salem M, Tsurusaki N, Divigalpitiya P (2019) Analyzing the driving factors causing urban expansion in the peri-urban areas using logistic regression: A case study of the greater Cairo region. Infrastructures 4(1). https://doi.org/10.3390/infrastructures4010004
101. Sarif MN, Siddiqui L, Islam MS, Parveen N, Saha M (2021) Evolution of river course and morphometric features of the River Ganga: A case study of up and downstream of Farakka Barrage. Int Soil Water Conserv Res 9(4):578–590. https://doi.org/10.1016/j.iswcr.2021.01.006
102. Sarkar A, Chouhan P (2020) Modeling spatial determinants of urban expansion of Siliguri a metropolitan city of India using logistic regression. Model Earth Syst Environ 6(4):2317–2331. https://doi.org/10.1007/s40808-020-00815-9
103. Simon A, Collison AJC (2002) Quantifying the mechanical and hydrologic effects of riparian vegetation on streambank stability. Earth Surf Proc Land 27(5):527–546. https://doi.org/10.1002/esp.325
104. Singh KV, Setia R, Sahoo S, Prasad A, Pateriya B (2015) Evaluation of NDWI and MNDWI for assessment of waterlogging by integrating digital elevation model and groundwater level. Geocarto Int 30(6):650–661. https://doi.org/10.1080/10106049.2014.965757
105. Singh M, Sinha R, Tandon SK (2020) Geomorphic connectivity and its application for understanding landscape complexities: a focus on the hydro-geomorphic systems of India. Earth Surf Proc Land 0–2. https://doi.org/10.1002/esp.4945
106. Sinha R, Ghosh S (2012) Understanding dynamics of large rivers aided by satellite remote sensing: A case study from Lower Ganga plains, India. Geocarto Int 27(3):207–219. https://doi.org/10.1080/10106049.2011.620180
107. Sinha R, Sarkar S (2009) Climate-induced variability in the Late Pleistocene-Holocene fluvial and fluvio-deltaic successions in the Ganga plains, India: A synthesis. Geomorphology 113(3–4):173–188. https://doi.org/10.1016/j.geomorph.2009.03.011
108. Sinha R, Tandon S, Gibling M, Bhattacharjee P, Dasgupta A (2005) Late Quaternary geology and alluvial stratigraphy of the Ganga Basin. Himalayan Geol 26(1):223–240
109. Tarolli P, Sofia G (2016) Human topographic signatures and derived geomorphic processes across landscapes. Geomorphology 255:140–161. https://doi.org/10.1016/j.geomorph.2015.12.007
110. Thakur PK, Laha C, Aggarwal SP (2012) River bank erosion hazard study of river Ganga, upstream of Farakka barrage using remote sensing and GIS. Nat Hazards 61(3):967–987. https://doi.org/10.1007/s11069-011-9944-z
111. Tipa G (2009) Exploring Indigenous Understandings of River Dynamics and River Flows: A Case from New Zealand. Environ Communication 3(1):95–120. https://doi.org/10.1080/17524030802707818
112. Ullah H, Islam MN, Malak MA (2016) Charland Dynamics of the Brahmaputra-Jamuna River in Bangladesh. Jahangirnagar Rev XXXIV(June):165–182
113. Vakhshoori V, Zare M (2018) Is the ROC curve a reliable tool to compare the validity of landslide susceptibility maps? Geomatics Nat Hazards Risk 9(1):249–266. https://doi.org/10.1080/19475705.2018.1424043
114. Vanhellemont Q (2020) Combined land surface emissivity and temperature estimation from Landsat 8 OLI and TIRS. *ISPRS Journal of Photogrammetry and Remote Sensing*, *166*(December 2019), 390–402. https://doi.org/10.1016/j.isprsjprs.2020.06.007
115. Verburg PH, Veldkamp A, Bouma J (1999) Land use change under conditions of high population pressure: The case of Java. Glob Environ Change 9(4):303–312. https://doi.org/10.1016/S0959-3780(99)00175-2
116. Wear DN, Bolstad P (1998) Land-use changes in Southern Appalachian landscapes: Spatial analysis and forecast evaluation. Ecosystems 1(6):575–594. https://doi.org/10.1007/s100219900052
117. Wohl E (2020) Rivers in the Anthropocene: The U.S. perspective. *Geomorphology*, *366*(xxxx). https://doi.org/10.1016/j.geomorph.2018.12.001
118. Yilmaz I (2009) Landslide susceptibility mapping using frequency ratio, logistic regression, artificial neural networks and their comparison: A case study from Kat landslides (Tokat-Turkey). Comput Geosci 35(6):1125–1138. https://doi.org/10.1016/j.cageo.2008.08.007

119. Zhang Z, Tan S, Tang W (2015) A GIS-based spatial analysis of housing price and road density in proximity to urban lakes in Wuhan City, China. Chin Geogra Sci 25(6):775–790. https://doi.org/10.1007/s11769-015-0788-4

120. Zhang, Z., Tan, S., & Tang, W. (2015). A GIS-based spatial analysis of housing price and road density in proximity to urban lakes in Wuhan City, China. *Chinese Geographical Science*, *25*(6), 775–790. https://doi.org/10.1007/s11769-015-0788-4

Tables

Table 1 is available in the Supplemental Files section.

Table 2 List of the variable included in the logistic regression model.

Variable type	Description	Code	Nature
Dependent variable	High Bank Erosion (1)	y	Categorical
	Low Bank Erosion (0)	y	
Predictor variables	NDVI	X1	Continuous
	MNDWI	X2	Continuous
	SAVI	X3	Continuous
	NDMI	X4	Continuous
	Distance to river	X5	Continuous
	Distance to settlement	X6	Continuous
	Population density	X7	Continuous
	Soil Dry Density	X8	Continuous
	Soil Bearing Capacity	X9	Continuous
	Land use-cover values	X10	Categorical

Table 3 Logistic regression model summary.

-2 Log likelihood	Cox & Snell R Square	Nagelkerke R Square	Hosmer-Lemeshow test		
381.306	.382	.525	Chi-square	df	Sig.
			4.335	8	.826

Table 4 Role of predictor variables in BLR model.

Predictor Variables	b	SE	Wald Statistics	df	Sig.	Exp(B)
NDVI	-1.569	1.615	0.943	1	0.332	0.203
MNDWI	1.571	1.899	0.684	1	0.408	4.81
MSAVI	0.325	1.149	0.08	1	0.777	1.384
NDMI	-1.759	2.066	0.725	1	0.395	0.172
Distance from river	-1.039	0.204	26.011	1	0.000	0.354
Distance from settlement	-0.164	0.166	0.972	1	0.324	0.849
Population density	-0.391	0.131	8.853	1	0.003	0.677
Soil dry density	5.746	3.56	2.605	1	0.107	312.966
Soil bearing capacity	-2.088	0.582	12.88	1	0.000	0.124
Swamp tracts & wetlands	.721	0.198	13.223	7	0.054	3.124
Settlement	0.813	0.521	2.437	1	0.118	2.254
Abandoned channels	0.763	1.397	0.298	1	0.585	2.145
Agricultural fields	1.523	0.514	8.789	1	0.003	4.585
Barren lands	0.84	0.4	4.413	1	0.036	2.317
Channel deposition	0.43	0.699	0.378	1	0.539	1.537
River channels	1.778	0.531	11.195	1	0.001	5.92
Mango plantation	-0.135	1.248	0.012	1	0.914	0.873
Constant	-2.978	1.539	3.747	1	0.043	0.051

Table 5 Details of the landuse-cover categories (2020).

LULC categories	Pixels	Area in Square Km	Area in %	Kappa coefficient
River channel	119081	107.32	9.175	0.765
Channel deposition	48458	40.13	3.430	
Abandoned channels	40461	34.03	2.909	
Swamp tracts & Wetlands	221191	57.72	4.934	
Barren soil	162840	143.02	12.227	
Agricultural fields	228141	336.3	28.751	
Mango plantations	333494	322.02	27.530	
Settlements	147582	129.13	11.039	

Table 6 Population pressure on the adjacent mouzas and change.

Sl. No.	GP[a]	Blocks	Population in 2001[b]	Population in 2011[c]	Increment	Remark
1	Dharampur	Manikchak	2798	3708	910	Outer bend erosion
2	Gopalpur	Manikchak	7072	9867	2795	along the left bank
3	Jotbhabani	Manikchak	2285	2582	297	
5	Panchanandapur	Kaliachak-II	21017	26358	5341	
6	Jotkasturi	Kaliachak-II	4491	4901	410	
8	Binodpur	Englishbazar	543	595	52	
9	Milki	Englishbazar	9516	12581	3065	

[a] Gram panchayet; Primary Census Abstract, DSH, Malda, [b]2001 & [c]2011, GoI

Figures

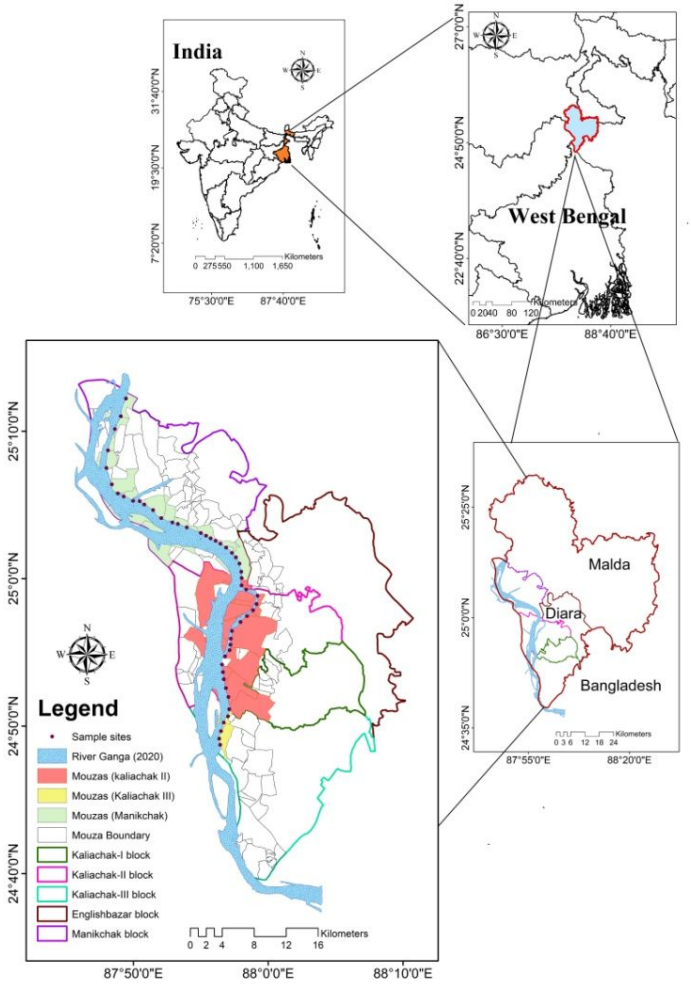

Figure 1

Study site location emphasizing Diara alluvial tract with mouza boundaries and selected sample sites along the left bank of Ganga.

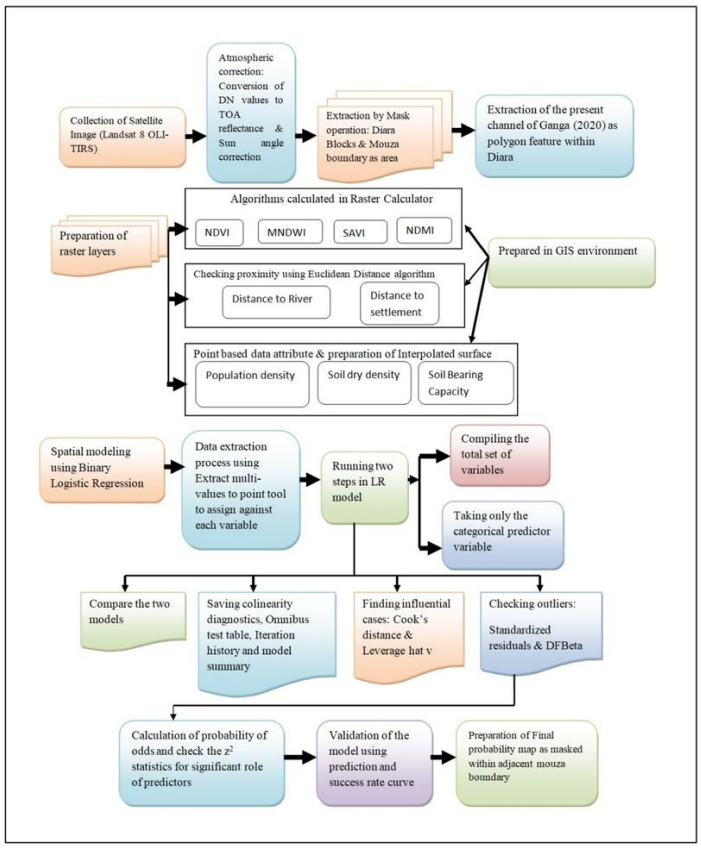

Figure 2

Methodological work flow of the present study.

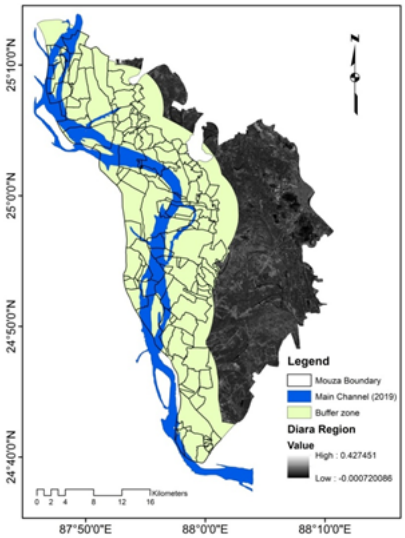

Figure 3

Extent of the study area within selected buffer of 5 km

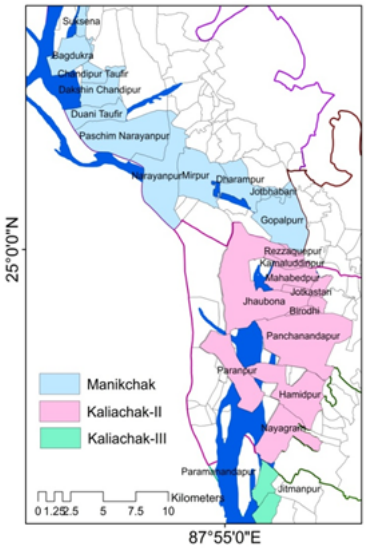

Figure 4

Bank erosion affected mouzas in Diara region

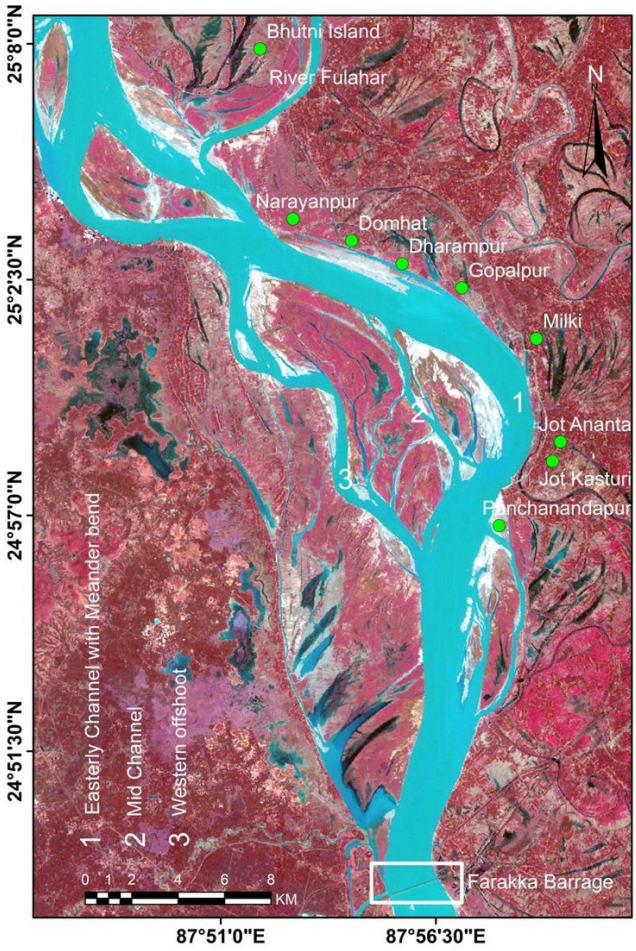

Figure 5

False Colour Composite of Landsat 8 (OLI/TIRS) data showing the channel configuration of Ganga in 2020 and potential bank erosion sites along the meander bend in Diara region (Malda district).

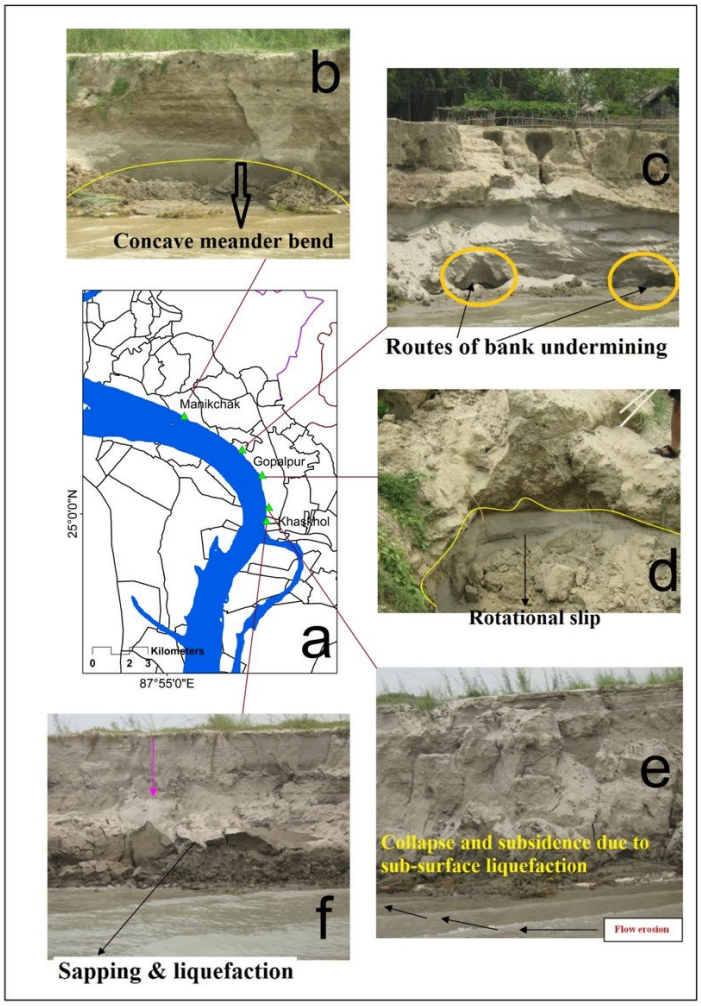

Figure 6

Field evidences of high bank erosion at the outer bend in Manikchak & Kaliachak-II blocks of Diara region.**a)** sites of field photographs; **b)**toe erosion causes concave bend near Domhut (Manikchak ghat);**c)** gullying and piping erosion through seepage on the areal collapse blocks of bank segments at Manikchak & Dharampur mouza;**d)** semi-circular rotational slip scars on the bankwalls at Gopalpur;**e)** vertical bank collapse at Khaskhol; **f)** Basal sapping and liquefaction dominated vertical bank slip at Khaskhol.

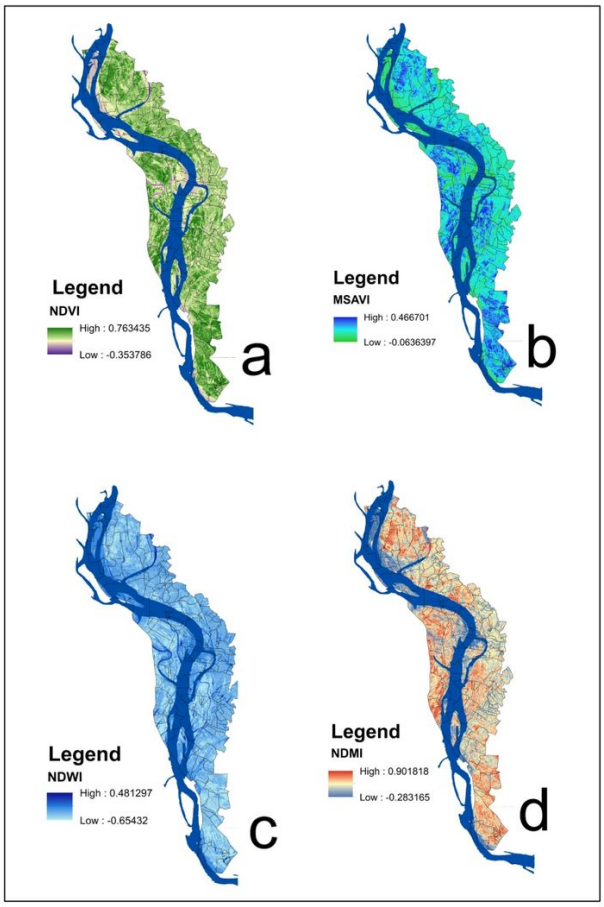

Figure 7

Predictor variables in the model.**a)** NDVI, **b)** MSAVI, **c)** NDWI, **d)** NDMI.

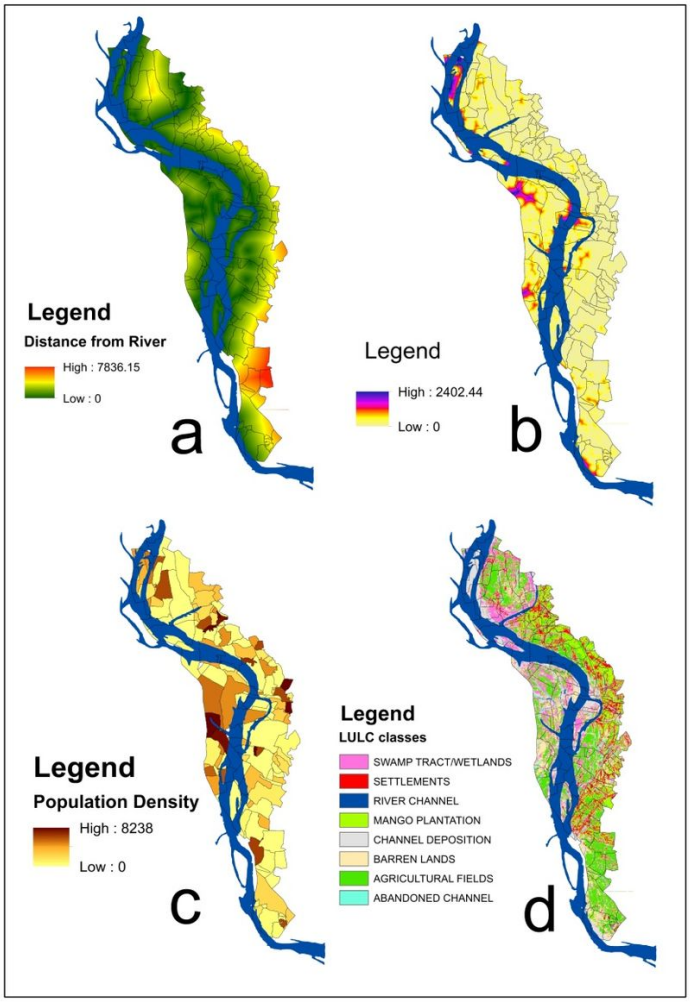

Figure 8

Predictor variables in the model. **a)** Distance to river;**b)** Distance to settlement;**c)** Population density;**d)** LULC categories.

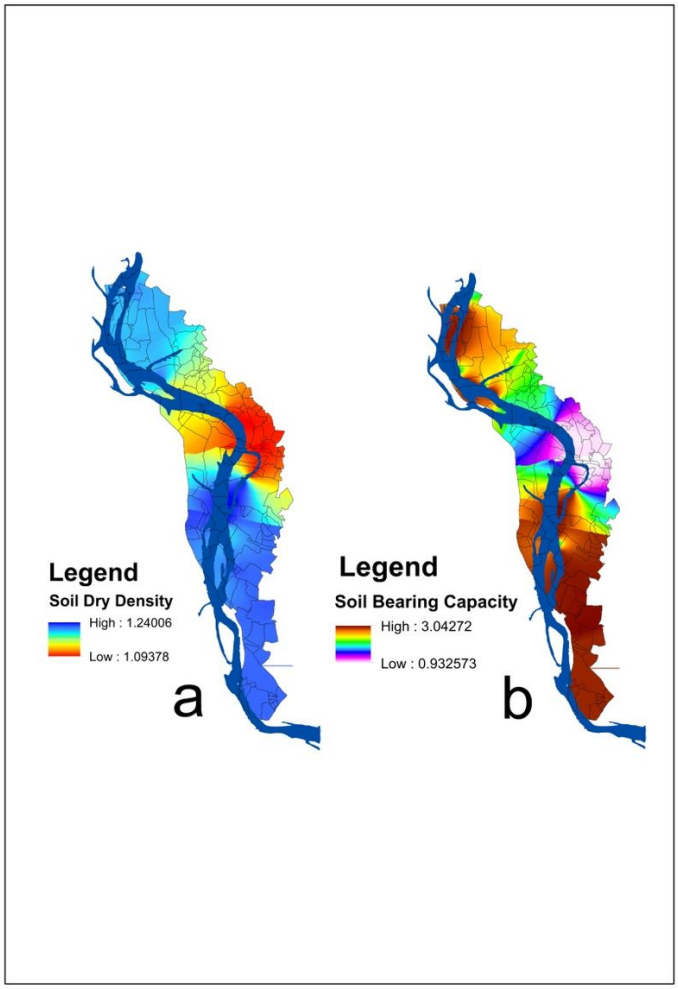

Figure 9

Spatial distribution of soil parameters. **a)** soil dry density; b**)** soil bearing capacity.

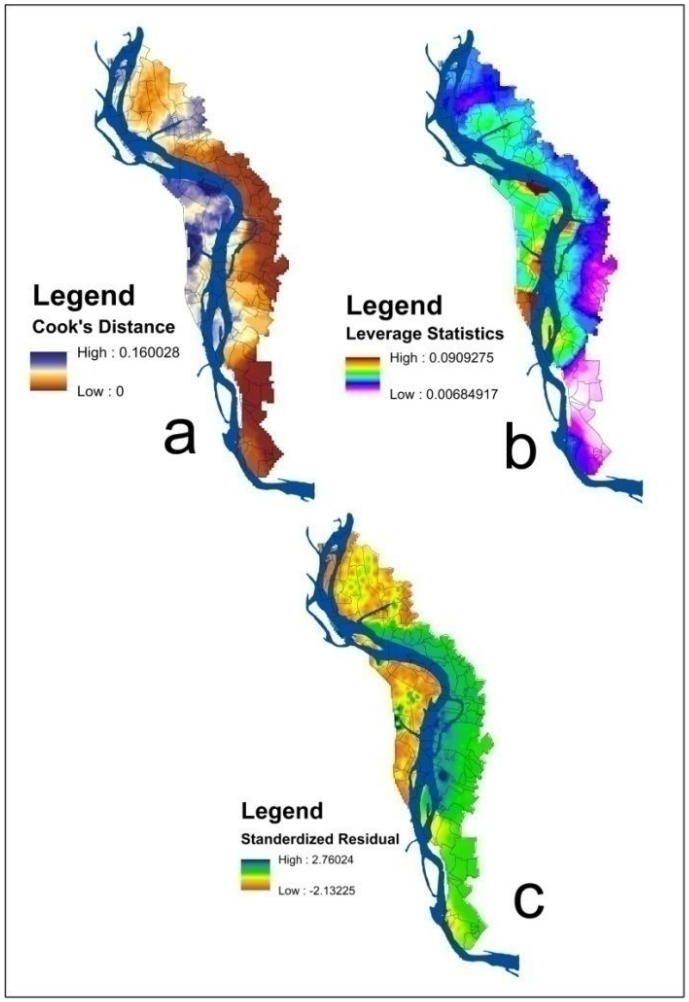

Figure 10

Residuals of the model; **a)** cook's distance; **b)** leverage statistics; c**)**standardized residuals.

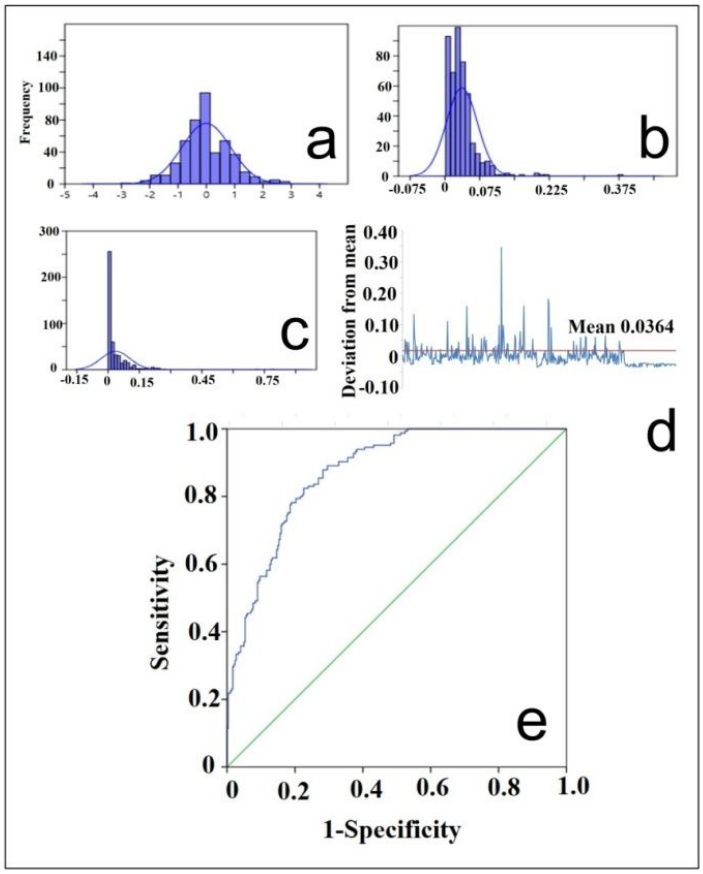

Figure 11

Frequency distribution of residuals & model validation. **a)** standardized residuals, **b)** Leverage statistics, **c)** Cook's distance; **d)** ROC curve.

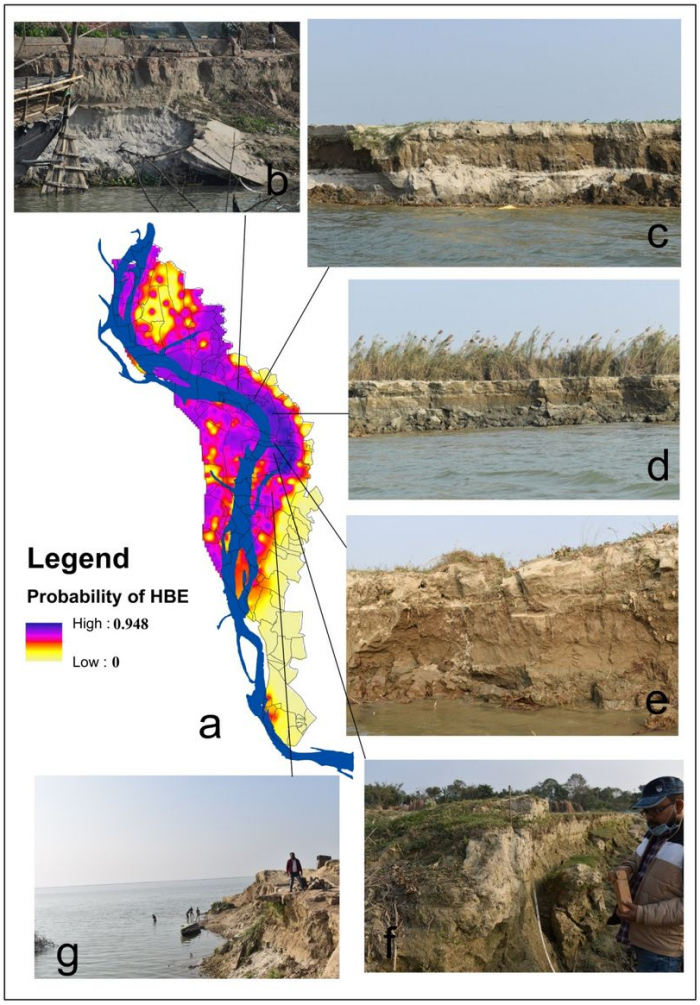

Figure 12

Validating the model with final outcome and recent (2020) field evidences. **a)** Variation of probability scores of bank erosion, **b)** erosion of unconsolidated sand both by recession of flood water and anthropogenic activities at Dharampur mouza, **c)** vertical block collapse and exposed bank face with three layers of deposition at Jotbhabani mouza, **d)** concave meander bend at Gopalpur mouza, **e)** Impinge flow attack and toe erosion at Kamaluddinpur mouza, **f)** Hydraulic wash out and toppling at Mahadebpur mouza & **g)** collapse and subsidence due to sub-surface liquefaction.

Supplementary Files

This is a list of supplementary files associated with this preprint. Click to download.

- Table1.docx